Partial entrainment of gravel bars during floods

Christopher P. Konrad
U.S. Geological Survey, Tacoma, Washington, USA

Derek B. Booth and Stephen J. Burges
Department of Civil and Environmental Engineering, University of Washington, Seattle, Washington, USA

David R. Montgomery
Department of Earth and Space Sciences, University of Washington, Seattle, Washington, USA

Received 6 August 2001; revised 14 January 2002; accepted 24 January 2002; published 11 July 2002.

[1] Spatial patterns of bed material entrainment by floods were documented at seven gravel bars using arrays of metal washers (bed tags) placed in the streambed. The observed patterns were used to test a general stochastic model that bed material entrainment is a spatially independent, random process where the probability of entrainment is uniform over a gravel bar and a function of the peak dimensionless shear stress τ_0^* of the flood. The fraction of tags missing from a gravel bar during a flood, or partial entrainment, had an approximately normal distribution with respect to τ_0^* with a mean value (50% of the tags entrained) of 0.085 and standard deviation of 0.022 (root-mean-square error of 0.09). Variation in partial entrainment for a given τ_0^* demonstrated the effects of flow conditioning on bed strength, with lower values of partial entrainment after intermediate magnitude floods ($0.065 < \tau_0^* < 0.08$) than after higher magnitude floods. Although the probability of bed material entrainment was approximately uniform over a gravel bar during individual floods and independent from flood to flood, regions of preferential stability and instability emerged at some bars over the course of a wet season. Deviations from spatially uniform and independent bed material entrainment were most pronounced for reaches with varied flow and in consecutive floods with small to intermediate magnitudes. *INDEX TERMS:* 1815 Hydrology: Erosion and sedimentation; 1821 Hydrology: Floods; 1869 Hydrology: Stochastic processes; *KEYWORDS:* sediment transport, bed material entrainment, disturbance, gravel bars, stochastic model

1. Introduction

[2] The entrainment of streambed material is a principal ecohydrologic process that influences fluvial sediment transport rates and the diversity and abundance of benthos in stream ecosystems. The spatial extent of bed material entrainment during a flood varies from a few grains to all of the material forming the bed surface, with correspondingly vast differences in sediment transport rates and biological consequences. Our objectives are to develop a relation between the fraction of a streambed surface entrained during a flood, which we refer to as partial entrainment, and the peak dimensionless shear stress during the flood and to evaluate whether bed material entrainment can be represented as a spatially independent, random process where the probability of entrainment is uniform over a gravel bar.

[3] Spatial distributions of the shear stress applied by streamflow τ and the critical shear stress of bed material τ_{cr} produce partial entrainment when τ exceeds τ_{cr} at some but not all locations on the bed [*Lane and Kalinske*, 1940; *Grass*, 1970]. Field studies using tracer particles and bed load samplers have demonstrated that partial entrainment rather than complete mobilization of a streambed prevails during most floods in gravel bed streams [*Andrews and Erman*, 1986; *Ashworth and Ferguson*, 1989; *Andrews*, 1994]. Flume investigations of the initial motion and transport rates of sediments also have documented the partial entrainment of sand and gravel beds [*Gilbert*, 1914; *Gessler*, 1970; *Grass*, 1970; *Wilcock and McArdell*, 1997]. In a study of six gravel bed streams, *Lisle et al.* [2000] conclude that only a limited portion of the streambed actively contributes sediment to bed load transport at bank-full discharge and that differences in the area of active transport reflects differences in sediment supply between the streams.

[4] Partial entrainment has been described as a stochastic process because there is a finite probability that the τ exceeds τ_{cr} at any location on a streambed due to temporal fluctuations in stream velocity [*Einstein*, 1942]. In a stochastic bed load transport model, *Einstein* [1942, 1950] used a Gaussian distribution to calculate the "instantaneous" probability of entrainment, based on a diffusion model for the spatial correlation of fluid velocity in turbulent flow [*Taylor*, 1935]. To calculate transport rates over larger reach scales encompassing many individual particles, Einstein equated the area entrained by streamflow to the probability of entrainment. *Lane and Kalinske* [1940] and *Grass* [1970] recognized partial entrainment as the area of streambed

0043-1397/02/2001WR000828$09.00

where τ exceeds τ_{cr}. Using a flume with a sand bed, Grass found that τ had positively skewed, unimodal probability distributions, while τ_{cr} had relatively uniform probability distributions. Although *Kirchner et al.* [1990] described the components influencing τ_{cr} (i.e., friction angle, projection, and exposure) as having widely distributed values for a water-worked bed, they did not suggest a general form for the distribution of τ_{cr}.

[5] In contrast to efforts to determine the individual distributions of τ and τ_{cr}, observations of bed mobility in flumes have been used to assess their joint distribution in terms of the probability of entrainment or partial entrainment. *Gessler* [1970] found that the cumulative probability that a particle remained on the bed surface during clear-water flume runs was normally distributed with respect to τ_{50i}/τ, where τ_{50i} is the shear stress that entrains 50% of the surface particles of size class i. In a sediment-recirculating flume, *Wilcock* [1997] observed that the equilibrium mobile fraction Y of any size class i had a log normal distribution with respect to τ/τ_{50i}. In both of these examples, the partial entrainment of a mixed sediment depends on the relative mobility of each particle size class.

[6] The applicability of entrainment theory [*White*, 1940; *Komar and Li*, 1986] or empirical results from flume experiments [see also *Little and Mayer*, 1976; *Fenton and Abbot*, 1977; *Ikeda and Iseya*, 1988] to gravel bed streams is difficult to confirm because of sparse data on the spatial distributions of τ and τ_{cr} and a lack of control on the processes and conditions in the field. However, if the probability of bed material entrainment is spatially uniform and independent over time, it could be estimated for a gravel bed stream with few data, facilitating the assessment of the sediment supply for bed load transport or the spatial extent of disturbance during floods.

2. Field Sites

[7] Spatial patterns of bed material entrainment were documented during floods at seven gravel bars in three streams (Jenkins, May, and Swamp Creeks) in the Puget Lowland, Washington (Figure 1). The basins draining to these creeks have intermediate levels of urban development but contrasting physiographic conditions and different hydrologic characteristics. As a result, these streams span much of the range of conditions that influence the relative sediment supply and transport capacity of gravel bed streams in the Puget Lowland region.

[8] All sites are in straight sections of pool-riffle or plane bed reaches [*Montgomery and Buffington*, 1997] with mid-channel or transverse gravel bars (of low amplitude in plane bed reaches) where the particle size distributions of bed material are relatively homogeneous and hydraulic conditions are relatively uniform (Table 1). Gravel bars are defined here as local in-channel deposits of gravel that rise above the mean profile of the bed surface [*Church and Jones*, 1982].

[9] Jenkins Creek drains a 37-km^2 basin on a glacial outwash plain. The mean discharge rate during water years (WY) 1989–1998 was 1.1 m^3 s^{-1} at the King County gage near its mouth. Storm flow recession is gradual, and base flows are high relative to other streams in the region.

[10] The supply of sediment to Jenkins Creek is limited by the presence of lakes and wetlands in the channel network and low rates of sediment delivery from hillslopes. The bar material in Jenkins Creek generally is well-sorted, imbricated gravels with a closed bed structure [*Laronne and Carson*, 1976]. Particles are well rounded, with a Corey shape factor (CSF) of ~0.6 (moderately flattened spheriods). The median diameter of bar material ranges from 30 to 48 mm. The texture and structure of the bar material are likely results of the sustained periods of flows competent to transport sand and small gravel in Jenkins Creek along with the low rates of sediment delivery to the channel.

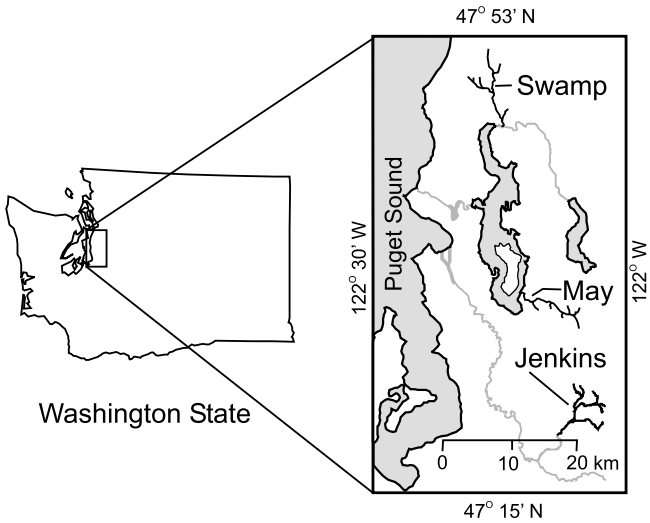

Figure 1. Streams where bed tag experiments were conducted in the Puget Lowland, Washington.

[11] Two gravel bars (A and B) were monitored in Jenkins Creek (Figure 2). The bars are 1 km apart without any major intervening tributaries. Jenkins Creek A is a midchannel bar in a straight reach that has a consistently low gradient of ~0.004 at low and intermediate stages. The water surface slope in the reach declined to ~0.001 during the largest observed floods. Jenkins Creek B is a transverse bar in a steeper reach. The water surface slope ranged from 0.016 at low stages to 0.006 at high stages. The bar has coarser gravel and lower amplitude than Jenkins A. There is a long radius meander bend upstream of this riffle and a concrete box culvert downstream. The meander bend does not generate a strong secondary (cross stream) flow pattern. The culvert exerts a hydraulic control at high stages backing water up to the downstream end of the bar.

[12] May Creek drains a 32-km^2 basin with steep headwaters and extensive glacial till deposits. The mean discharge rate during WY 1989–1998 was 0.7 m^3 s^{-1} at the King County gage (37A) near its mouth. In contrast to Jenkins Creek, May Creek has relatively high peak discharge rates during storms, rapid recession rates, and low base flow.

[13] Steep hillslopes along the channel and high-gradient tributaries contribute sediment to May Creek. Bed material on the bars in May Creek is poorly sorted gravel with a large fraction of sand and finer material and, in some cases, bimodal particle size distributions. Bars in May Creek have more open structure than Jenkins Creek with many particle clusters [*Brayshaw et al.*, 1983]. Bar material is slightly more angular than in Jenkins Creek with a CSF of ~0.5 and

Table 1. Physical Characteristics of the Experimental Sites[a]

Field Site	Channel Width, m	Bar Length, m	Bar Amplitude, m	Water Surface Slope (Low Flow–High Flow)	Surface Particle Size Distribution, mm			Channel and Sediment Characteristics
					D_{10}	D_{50}	D_{90}	
				Jenkins Creek				
Bar A	10.5	23	0.5	0.004–0.001	5	30	68	pool-riffle channel; well-sorted armor layer over bimodal gravel-sand mixture
Bar B	7.0	24	0.3	0.016–0.006	11	48	111	pool-riffle channel; armored gravel
				May Creek				
Bar A	10.0	45	0.6	0.006–0.011	6	40	95	plane bed channel; poorly sorted gravel armor over bimodal gravel-sand mixture
Bar B	9.0	35	0.5	0.008–0.016	8	31	88	pool-riffle channel; poorly sorted gravel armor over bimodal gravel-sand mixture
Bar Z	9.0	34	0.2	0.016–0.011	10	50	135	pool-riffle channel; armored gravel
				Swamp Creek				
Bar A	5.0	16	0.1	0.003–0.012	4	48	130	plane bed channel; poorly sorted gravel over coarse subsurface material
Bar B	9.0	45	0.2	0.002–0.007	3	19	45	pool-riffle channel; gravel armor over bimodal gravel-sand mixture

[a] Bar length was measured from the deepest point of the pools upstream and downstream of the bar. Bar amplitude was measured as the maximum height between the bar surface and a line drawn from the deepest points of the upstream and downstream pools.

with median diameters ranging from 31 to 50 mm. The texture and structure of bed material in May Creek are likely a consequence of a large sediment supply and short duration of flows that are able to sort bed material.

[14] Three gravel bars (A, B, and Z) were monitored in May Creek. May A is a transverse gravel bar with a steep, foreset slope leading to a pool formed at a meander bend (Figure 3a). The upstream end of the bar is ill defined in a plane-bed reach. The water surface slope in May A ranges from 0.011 at low stages to 0.006 at high stages due to the backwater created by the downstream bend. May B is a transverse bar located 200 m downstream from May A (Figure 3b). The water surface slope in this reach ranges from 0.008 at low stages to 0.016 at high stages. May Z is a transverse bar in a relatively straight, pool-riffle reach (Figure 3b) upstream of May A and B. The water surface slope ranges from 0.016 at lower stages to 0.011 at higher stages.

[15] Swamp Creek drains a 59-km^2 basin comprising a glacial till plateau. The mean discharge rate during WY 1989–1998 was 0.4 m^3 s^{-1} at the Snohomish County gage (drainage area = 25 km^2). The U.S. Geological Survey operated a gage (12127100) near the mouth of Swamp Creek where the mean discharge rate was 1.0 m^3 s^{-1} during WY 1980–1989. The hydrologic regime of Swamp Creek falls between that of Jenkins and May Creeks with intermediate peak flows and recession rates, though it has the highest frequency of storm events.

[16] The sediment supply is relatively limited in Swamp Creek, particularly in the upper basin, which has large, in-channel wetlands. Bar material in the upper reaches is poorly sorted with very large cobbles (>0.3 m diameter) lying beneath the gravel surface layer. The lower reaches of Swamp Creek have low gradients and, consequently, low capacity to transport sediment and therefore finer bed material distributions. Bar surfaces generally have a closed structure in Swamp Creek with more imbricated clasts in the upper reaches and loosely packed clasts in the lower reaches. Bar material is well rounded, with a CSF of ~0.5 and median diameters ranging from 19 to 48 mm.

[17] Two gravel bars were monitored in Swamp Creek (Figure 4). Swamp Creek A is a midchannel bar located 100 m upstream of the active stream gage. The channel is straight with uniform width, a nearly plane bed, and low-amplitude bars. The water surface slope ranges from 0.003 at low stages to 0.012 at high stages. Swamp Creek B is a midchannel bar located in a lower gradient pool-riffle reach that was reconstructed circa 1996 including the reestablishment of a meandering planform, placement of large woody debris along the channel margins to deflect flow, construction of a low levee along the left bank, and riparian plantings. The water surface slope ranges from 0.002 at low stages to 0.007 at high stages.

3. Methods for Documenting Bed Material Entrainment

[18] Patterns of bed material entrainment were documented at seven gravel bars using arrays of bed tags. Bed tags are steel washers (38 mm diameter, 2 mm thick) with a short length (<5 cm) of plastic flagging. Each tag was inserted vertically between the particles forming the streambed surface with its axis oriented cross stream until its top was flush with the point of contact of the particles forming the bed surface (Figure 5). Placed in this manner, tags did not induce local scour and remained immobile unless the particles forming the surface of the bed were entrained. The tags were dislodged when the adjacent surface particles moved during a flood. Tags generally were not recovered after they were displaced by floods.

[19] A bed tag is supported by the contact between two or more adjacent particles forming the surface of the streambed

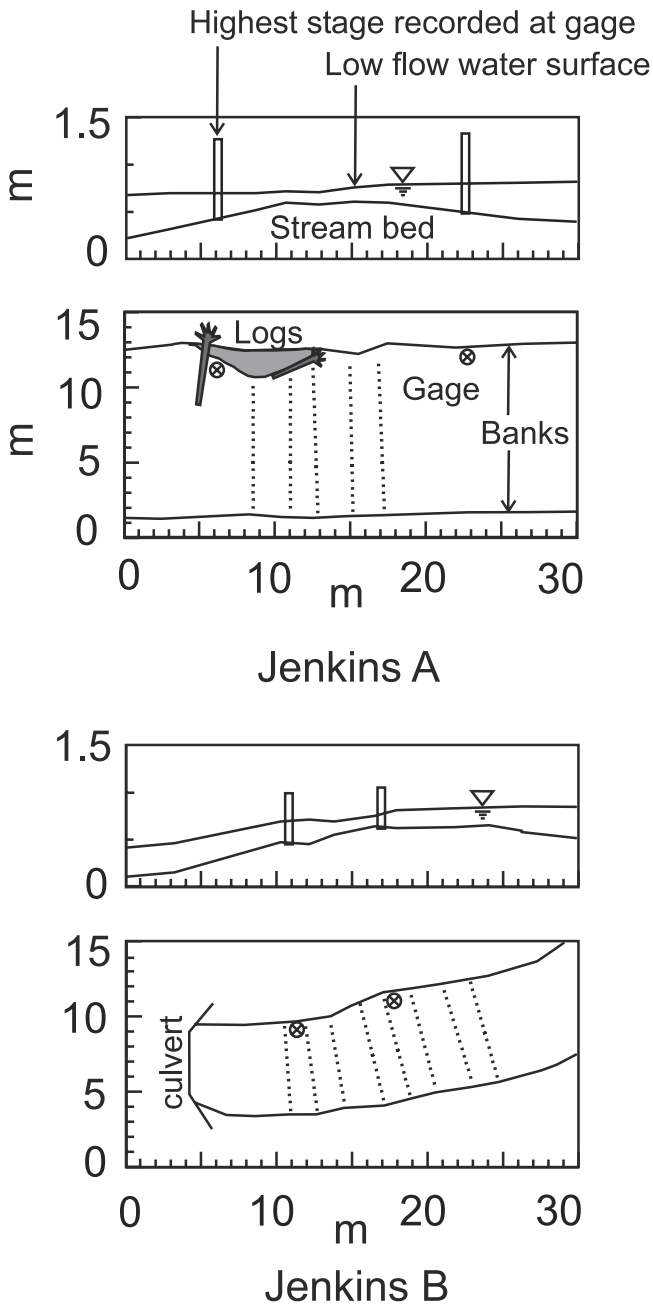

Figure 2. Longitudinal profiles and plan views of sites in Jenkins Creek with bed tags (ticks).

and only indicate the movement of these particles. Thus bed tags do not indicate the movement of nonadjacent particles or small particles that do not support the bed tag but, nonetheless, may be next to it. These represent type 1 errors (a tag present but bed material was entrained). Type 1 errors resulting from spatially limited sampling are analyzed in the results of the bed tag inventories. Other type 1 errors were minimized through site selection by avoiding gravel bars where unconstrained particles form much of the bed surface or where the bed tags were much larger than particles forming the bed surface and, consequently, supported by many particles. Partial exposure of tags was not routinely observed at any of the sites. However, bed tags at the channel margins in two rows at May B and Swamp B were placed in fine-grained deposits of sand and gravel where bed material was occasionally entrained without dislodging the tags. In such cases of widely graded sediments, bed tags do not indicate low levels of bed material entrainment.

[20] Type 2 errors (a bed tag was missing but no bed material was entrained) occurred at a few locations in some

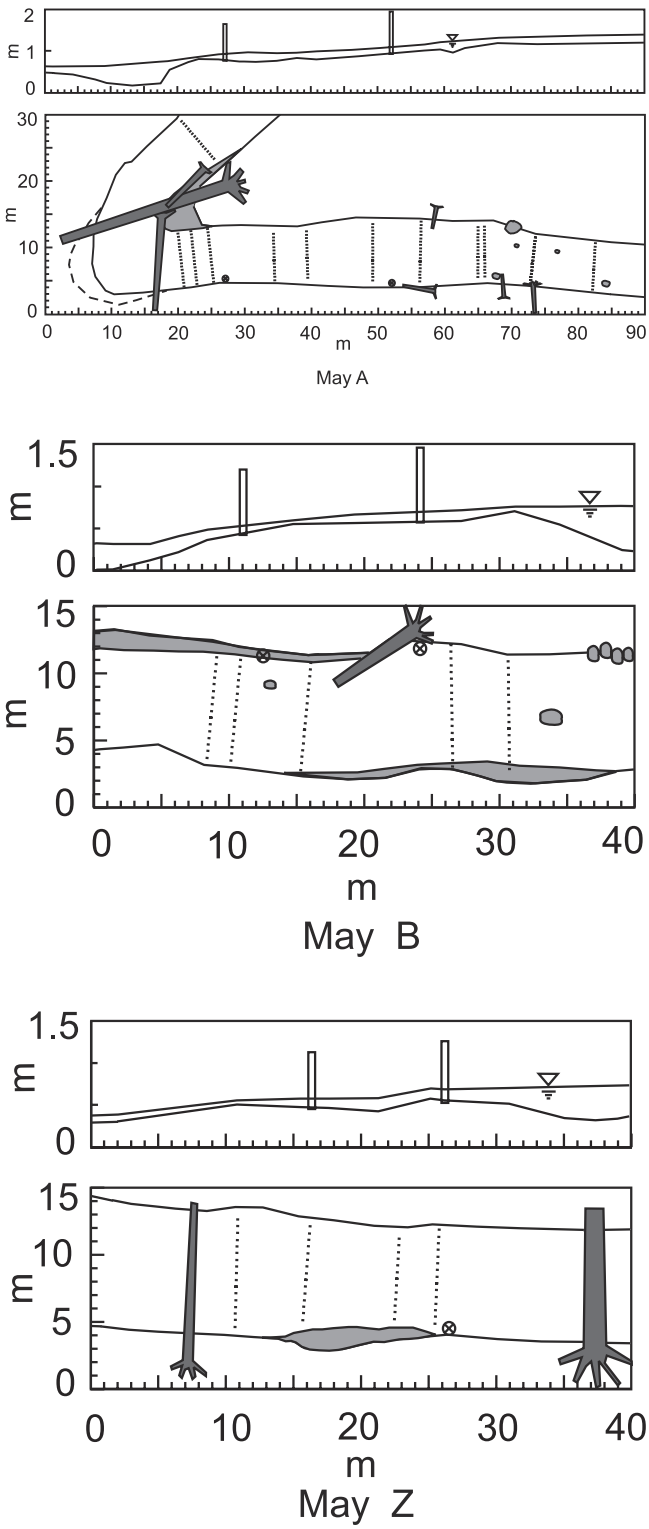

Figure 3. Longitudinal profile and plan view of May Creek sites.

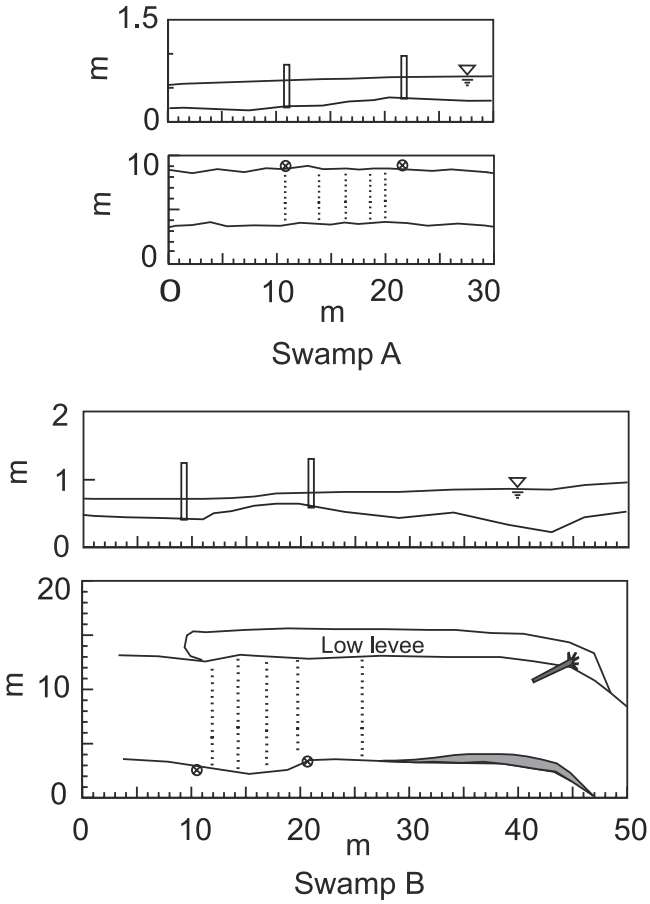

Figure 4. Longitudinal profiles and plan views of Swamp Creek sites.

inventories when a tag that appeared to be missing was actually buried. A buried tag was usually uncovered when a new tag was placed at that location, though occasionally a buried tag was found later in the season. In these cases, the last recorded instance when the tag was missing was revised to indicate that the tag had been present. The potential for errors resulting from the size of the bed tag or drag on the plastic flagging was assessed at two field sites using an alternative bed tag design. Plastic flagging attached to a 10-cm-long piece of metal wire bent into a "U" was inserted into the streambed, like a small croquet wicket, next to each metal washer type bed tag at the sites during two periods. The low weight of the wire tags and their small surface area in contact with bed material offered less resistance to entrainment. The two types of tags produced identical results (i.e., present or missing) at every location, demonstrating that entrainment of tags did not depend on the weight of the tag relative to the drag on the plastic flagging. We conclude that the weight of metal washers is unlikely to increase type 1 errors relative to those of the much lighter wire tags. Moreover, type 2 errors are unlikely where bed tags can be placed securely between particles in the streambed.

[21] At each site, the tags were placed at 0.5-m intervals across the stream channel in rows across the bars. A 30-cm steel spike was driven into the left stream bank at each row, and the first tag was located 1 m from the spike to ensure consistent tag locations over time and facilitate finding tags during high-flow periods when visibility was poor. The rows had between 9 and 21 tags depending on the width of the channel. There were four to eight rows of tags and 45 to 103 bed tags at each bar. The rows spanned the channels from bank to bank except at the right end of Jenkins A, row 5, where the bed material was silt and fine organic debris rather than gravel. Large boulders were located at two locations (Swamp A, row 1, tag 9 and Swamp B, row 2, tag 1). Rather than placing tags at these boulders, the boulders were observed to be stable throughout the experiments.

[22] In addition to the five rows of bed tags on the May A gravel bar (rows 5, 6, 7, 8, and 10), seven rows of bed tags (rows 1, 2, 3, 4, 9, 11, and 12) were placed in the reach around the May A bar to characterize patterns of bed material entrainment associated with other channel forms. The observations of tags in these seven rows are excluded from the bar-scale results and are described only in section 7 in the context of the spatial variability in partial entrainment.

[23] The bed tags were inventoried on 103 occasions (every 1–4 weeks) at the seven gravel bars from October 1997 to December 1999. During the inventories the location (row and tag number) of each missing tag was recorded and the tag was replaced. The Eulerian experimental design allowed a time series of entrainment to be developed for each tag location. Generally, bed tags were inventoried after a single flood peak, with notable exceptions at the Swamp Creek sites (three peaks between the bed tag inventories on 16 November 1998 and 15 December 1998) and at the Jenkins Creek sites (two peak between 7 December 1998 and 4 January 1999). At each bar, there was at least one inventory when no tags had moved since the previous inventory, providing an estimate of the maximum value of τ_0^* at each site when the bed was stable.

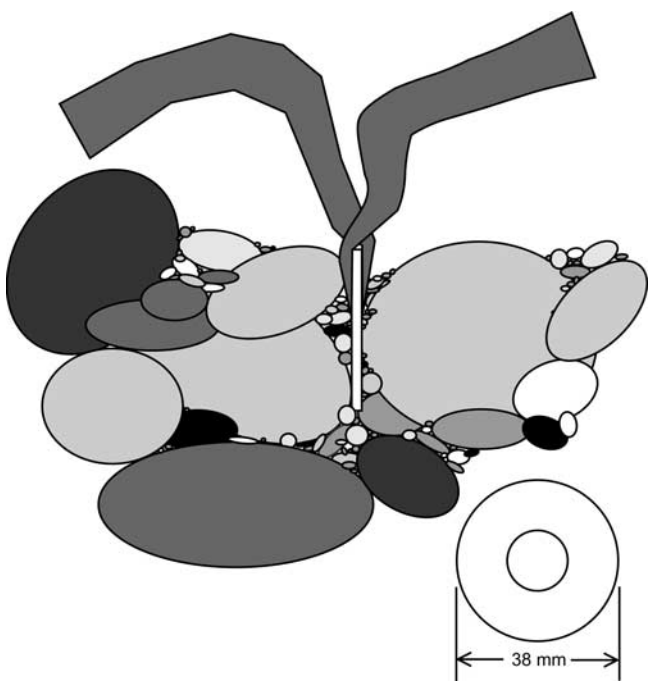

Figure 5. Cross section of bed tag in a streambed.

[24] The peak water stage between inventories was recorded at two crest stage gages separated by 10–20 m at the upstream and downstream ends of each gravel bar. The crest stage gages were constructed from steel rods (~1-cm diameter) driven into the streambed near the bank. Hook-and-loop fabric tape (Velcro®) was fastened along the exposed rod such that debris suspended in the streamflow (e.g., fine sediment, particulate organic material, and leaves) would collect in the hooks and loops leaving an easily identifiable high-water mark.

4. Analytical Methods and Calculations

4.1. Applied Shear Stress

[25] The distribution of τ varies over a streambed, typically with low values near stream banks and high values near the center of the channel [*Chow*, 1959, p. 169] as well as local influences from bed material or other flow obstructions [*Rouse*, 1965]. The total boundary shear stress τ_0 was used as a central measure of the distribution of the applied shear stress over a gravel bar. The total boundary shear stress along a reach with uniform flow is calculated as

$$\tau_0 = \gamma_w R S, \tag{1}$$

where γ_w is the specific weight of water, R is the hydraulic radius, and S is the calculated energy gradient of the streamflow along the bar.

[26] The peak total boundary shear stress τ_0 was calculated with equation (1) for each period between inventories. R was calculated as the wetted cross-sectional area divided by the wetted perimeter at the surveyed section using the maximum stage recorded between each inventory. The energy gradient for each flood at each site was estimated using the water surface slope between the two gages (Table 1). The slope calculation assumes that peak stage was synchronous at each gage. The error in water surface slopes is estimated to be at most ±0.001.

[27] In uniform flow, τ_0 is equal and opposite to all of the pressure and viscous forces on a unit bed area basis that resist the gravitational acceleration of water as it flows downstream. Here τ_0 includes form drag that acts over regions of flow separation larger than individual particles (around bends and over bars) without contributing to sediment transport and skin friction that acts at the scale of individual particles. Skin friction is the only component of τ_0 that transports sediment [*Einstein*, 1950; *Einstein and Barbarossa*, 1952; *Smith and McLean*, 1977; *McLean et al.*, 1999].

[28] Experimental sites were selected in straight reaches with few obstacles to minimize form drag; however, we did consider whether τ_0 provides a reasonable approximation of skin friction. Local skin friction τ_g can be estimated from the vertical velocity profile in a fully developed boundary layer (where the vertical velocity profile does not change in the stream-wise direction) using the Prandtl-Von Karman logarithmic velocity distribution [*Grass*, 1970; *Nece and Smith*, 1970; *Schlichting*, 1979; *Wilcock*, 1996]:

$$u(z) = \frac{u^*}{\kappa} \ln\left(\frac{z}{z_0}\right), \tag{2}$$

where $u(z)$ is the velocity at a height z above the bed, K = 0.41 is von Karman's coefficient, z_0 is the roughness length scale, and $u^* = (\tau_g/\rho)^{0.5}$ is the shear velocity associated with skin friction. Values of u^* estimated from equation (2) based on measured vertical velocity profiles were compared to $u_0^* = (\tau_0/\rho)^{0.5}$ for cross sections in Jenkins A, May A, and Swamp B.

[29] Current velocity was measured at Jenkins A, May B, and Swamp B with a Marsh-McBirney current meter at 10–25 positions across the channel at the highest flow when the streams could be safely waded. At each position, measurements were made at 1 cm above the bed and at 5-cm intervals up to the water surface. Shear velocity, $u^* = \mathrm{K}(u_1 - u_2)/\ln(z_1/z_2)$, was calculated using two velocity measurements (u_1 and u_2) in the near-bed region not more than 0.2 of flow depth above the bed, where current velocities are expected to vary logarithmically [*Wiberg and Smith*, 1991], notwithstanding the effects of large clasts preventing full development of the turbulent boundary layer.

[30] An example of the velocity profiles and a theoretical velocity distribution calculated from equation (2) assuming $u^* = u_0^*$ and $z_0 = 0.1D_{84}$ [*Whiting and Dietrich*, 1990] is shown for May A on 5 January 1998 (Figure 6). At May A, $u^* = 0.02 - 0.3$ m s^{-1} for the measured velocity profiles compared to $u_0^* = 0.22$ m s^{-1} calculated assuming for uniform flow. The value of u_0^* is higher than the value of u^* at 90% of the locations across the section. The estimates of u^* based on measured velocity gradients have limited accuracy because vertical velocity profiles are not strictly logarithmic over rough boundaries [*Grass*, 1971; *Wiberg and Smith*, 1991; *Pitlick*, 1992]. Furthermore, the velocities are mean values measured consecutively over at least a 1-min period, rather than simultaneous and instantaneous velocities, and are likely to have large relative errors for low values near the streambed.

[31] For any of the cross sections examined the vertical velocity gradients spanned a wide range of values with lower vertical velocity gradients near a channel's banks and steeper gradients in the center of the channel. Although most of the local values of u^* were less than u_0^*, the values of u^* in the center of the channel were higher than u_0^*. Accordingly, we recognize that τ_0 is only an index of the distribution of τ_g and, moreover, τ_0 is representative of only the highest values of τ_g across a channel.

4.2. Dimensionless Shear Stress

[32] The balance between the applied and resisting shear stresses is represented here by a dimensionless shear stress τ_0^*, which is the ratio of total boundary shear stress to an index of the unit area buoyant weight of the median of the particle size distribution:

$$\tau_0^* = \frac{\tau_0}{(\gamma_s - \gamma_w) D_{50}}, \tag{3}$$

where γ_s is the specific weight of the sediment and D_{50} is the median of the particle size distribution of the surface material. The reported values of τ_0^* at the threshold of motion (τ_{cr}^*) for gravel in a turbulent boundary layer span a wide range from 0.02 to 0.08 [*Fahnstock*, 1963; *Parker and Klingeman*, 1982; *Andrews*, 1983; *Andrews and Erman*,

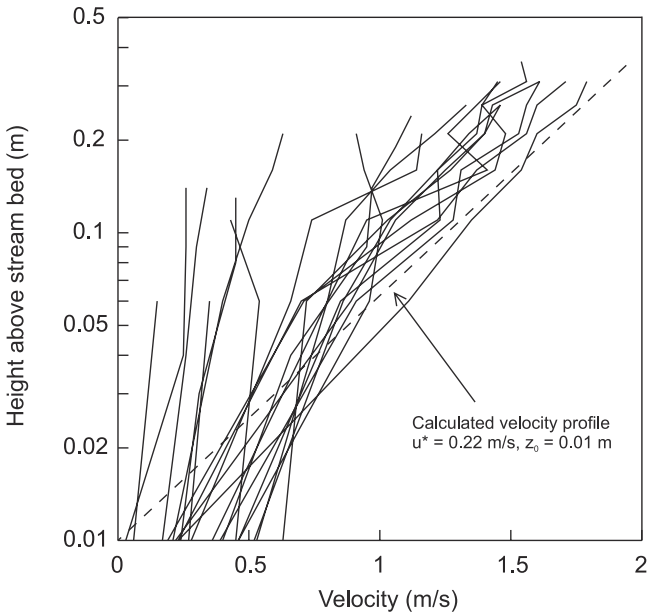

Figure 6. Measured velocity profiles (solid lines) at a cross section in May A with calculated velocity profile (dashed line) assuming $u^* = 0.22$ m s^{-1} and $z_0 = 0.01$ m.

1986; *Carling*, 1983, *Buffington and Montgomery*, 1997]. The range is partially an artifact of different criteria used to define initial motion from the first movement of one particle to the widespread entrainment of a bed's surface [*Gilbert*, 1914; *ASCE Task Committee on the Sedimentation Manual*, 1966]. *Neill and Yalin* [1969] proposed that a constant bed load transport rate should be the basis for a quantitative criterion of initial motion of a sediment. Area is used here as the basis for reporting bed material entrainment rather than a transport rate because the area of streambed entrained during a flood indicates the supply of material to bed load transport and the spatial extent of streambed disturbance during a flood.

[33] Dimensionless shear stress τ_0^* was calculated for each flood at each site with equation (3) using the median of the particle size distribution of the surface material of the bar. The particle size distributions of the bar surfaces were estimated using pebble counts [*Wolman*, 1954]. Each count included 100 particles plucked from the channel surface from an area ~5 m long and extending from bank to bank. Two to five pebble counts were conducted on each bar where bed tags were located. Pebble counts were conducted during low flow conditions in the spring and summer. The 10th, 50th, and 90th percentiles of the particle size distribution (D_{10}, D_{50}, and D_{90}) for the surface material of each gravel bar are listed in Table 1. The specific weight of the sediment in equation (3), $\gamma_s = 2700$ kg m^{-3}, was based on the average value for bulk samples collected from each creek.

[34] Estimates of τ_0^* from equation (3) have uncertainty resulting from errors in R, S, and D_{50}. Errors in R and S result from uncertainties in the field measurements of flood stage. Errors in D_{50} are a result of bias and error from using a pebble count to sample bed surface material [e.g., *Kellerhals and Bray*, 1971; *Hey and Thorne*, 1983; *Diplas and Sutherland*, 1988; *Wolcott and Church*, 1991]. A nonparametric 95% confidence interval around D_{50} was estimated using the 40th and 60th percentiles of the particle size distribution [*Helsel and Hirsch*, 1993, p. 70].

[35] The cumulative influence of the errors on calculated values of τ_0^* was estimated using a first-order approximation of the variance of τ_0^* is

$$\mathrm{Var}(\tau_0^*) \approx \left(\frac{\partial \tau_0^*}{\partial R}\right)^2_{\bar{R}} \mathrm{Var}(R) + \left(\frac{\partial \tau_0^*}{\partial S}\right)^2_{\bar{S}} \mathrm{Var}(S) + \left(\frac{\partial \tau_0^*}{\partial D_{50}}\right)^2_{\bar{D}_{50}} \mathrm{Var}(D_{50}) \; . \tag{4}$$

The first two terms on the right side of equation (4) are two orders of magnitude smaller than the last term. Consequently, the uncertainty associated with R and S was ignored, and the lower and upper bounds of the 95% confidence interval around D_{50} at each site were propagated through equation (3) to yield approximate 95% confidence intervals for τ_0^*.

4.3. Partial Entrainment and Probability of Entrainment

[36] Partial entrainment of a gravel bar during a flood was estimated as the fraction of bed tags missing from the bar (PE_{bar}) during the subsequent bed tag inventory. We assess uncertainty in the estimates of partial entrainment due to bed tag sampling error and analyze spatial and temporal patterns in partial entrainment using the cumulative binomial distribution function:

$$B(N) = \sum_{x=0}^{N} \frac{n!}{x!(n-x)!} p^n (1-p)^{n-x}, \tag{5}$$

where B is the likelihood of observing N or fewer bed tags missing from a sample of n tags with a uniform probability of entrainment p. Initially, equation (5) is applied at the scale of a bar ($N/n = PE_{bar}$) to assess bed tag sampling error and changes in the entrainment probability for a specific value of τ_0^* over time. Subsequently, equation (5) is applied to individual rows to identify those rows with significantly more or less extensive bed material entrainment than the bar ($N/n = PE_{row}$, $p = PE_{bar}$).

[37] Given the distribution of sedimentologic and hydraulic conditions over a streambed, the probability of entrainment will asymptotically approach 0 at low values of τ_0^* and 1 at high values of τ_0^*. The cumulative Gaussian distribution was used as an analytical function for estimating partial entrainment as a function of τ_0^*:

$$PE_{bar} = \int_0^{\tau_0^*} \frac{1}{\sqrt{2\pi}\sigma} \exp \frac{-(\tau_0^* - \tau_{50}^*)^2}{2\sigma^2} d\tau_0^* \; , \tag{6}$$

where τ_{50}^* is the mean value of the distribution (50% of a bar's surface is expected to be entrained at $\tau_0^* = \tau_{50}^*$) and σ is the standard deviation (16% of the bar's surface is expected to be entrained at $\tau_0^* = \tau_{50}^* - \sigma$, and 84% of the bar's surface is expected to be entrained at $\tau_0^* = \tau_{50}^* + \sigma$).

5. Results

[38] Floods produced a wide range in partial entrainment of the gravel bars during the study period. The most

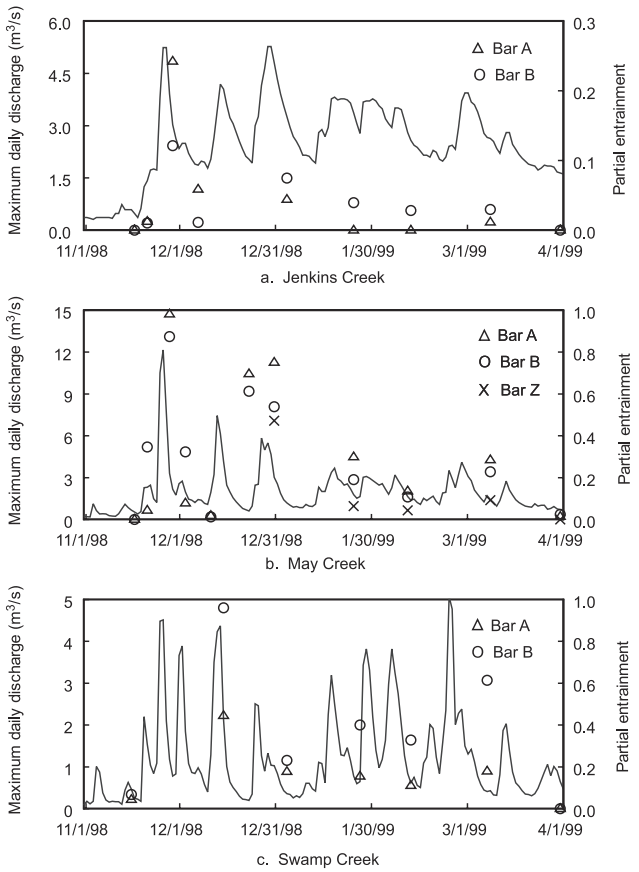

Figure 7. Maximum daily discharge Q_{max} and fraction of bed tags missing (PE_{bar}) from seven gravel bars during WY 1999.

frequent and extensive bed material entrainment occurred during water year 1999 at all of the sites (Figure 7). Bar surfaces were partially entrained over a range of τ_0^* from 0.026 to 0.12 (Figure 8). PE_{bar} varied directly with τ_0^* at all sites, though values of PE_{bar} were scattered over much of the observed range of τ_0^*. Partial entrainment was frequently <0.2 at all sites and exceeded 0.5 for inventories at only three sites: May A, May B, and Swamp B (Table 2).

[39] For a given flood, PE_{bar} varied among the bars but was relatively similar for the bars in each stream (Figure 7). The maximum PE_{bar} at all sites occurred between 21 and 28 November 1998 when the peak discharge rates were 12.5 $m^3\ s^{-1}$ (annual return period ~2.5 years) at May Creek, 5.3 $m^3\ s^{-1}$ (annual return period ~2.5 years) at Jenkins Creek, and 4.5 $m^3\ s^{-1}$ (annual return period ~1.2 years) at Swamp Creek. During this period, PE_{bar} varied considerably between streams, from 0.12 for Jenkins B to 0.98 for May A.

[40] The relation between PE_{bar} and τ_0^* was approximated with a cumulative Gaussian distribution function equation (6) with mean value of $\tau_{50}^* = 0.085$ (at which $PE_{bar} = 0.5$) and $\sigma = 0.022$ (Figure 9). The observed values of PE_{bar} have a root-mean-square error of 0.090 (corresponds to 9% of a bar's surface) when compared to calculated values from equation (6) using the above parameters. The differences between observed and calculated values of PE_{bar} reflect, in part, uncertainty associated with the calculated values of τ_0^* and the observed values of PE_{bar}. Examples of the ~95% confidence intervals calculated with equation (4) are shown in Figure 9 as horizontal error bars around some of the calculated values of τ_0^*. In general, we expect that the actual value of τ_0^* has a 95% probability of being between 74 and 117% of the calculated value.

[41] To assess the uncertainty in our observations of partial entrainment due to bed tag sampling error, we calculated 95% confidence intervals around observed values of PE_{bar} by solving the cumulative binomial distribution equation (5) in terms of p. There is a 5% probability that the actual partial entrainment of a gravel bar was outside of the calculated confidence interval. We set m equal to the number of missing tags ($m = nPE_{bar}$) and $B(m) = 0.025$ for the upper bound (i.e., the highest value of p for which PE_{bar} was likely to be observed) and $B(m) = 0.975$ for the lower bound (i.e., the lowest value of p for which PE_{bar} was likely to be observed). The 95% confidence intervals for selected PE_{bar} observations are shown as vertical error bars in Figure 9. The potential sampling error is greatest when the probability of entrainment is 0.50, in which case 95% of the observed values of PE_{bar} are expected to be between 0.37 and 0.63 (i.e., 0.50 ± 0.13).

[42] Some of the observed data are unlikely to be represented by the theoretical distribution as indicated by those points where the measurement error bars do not extend to the line in Figure 9. These observations may deviate from the theoretical distribution because of measurement errors exceeding the estimated confidence intervals, stochastic entrainment of bed material not related to τ_0^*, or changes in the strength of the bar surfaces between inventories. These factors are analyzed below in terms of variation in the threshold of entrainment at a bar (section 5.1) and variation in partial entrainment at a bar for a given shear stress (section 5.2).

5.1. Variation in the Threshold of Entrainment Between Inventories at a Bar

[43] The threshold for bed material entrainment (τ_{cr}^*) varied over time at all bars: the maximum value of τ_0^* at

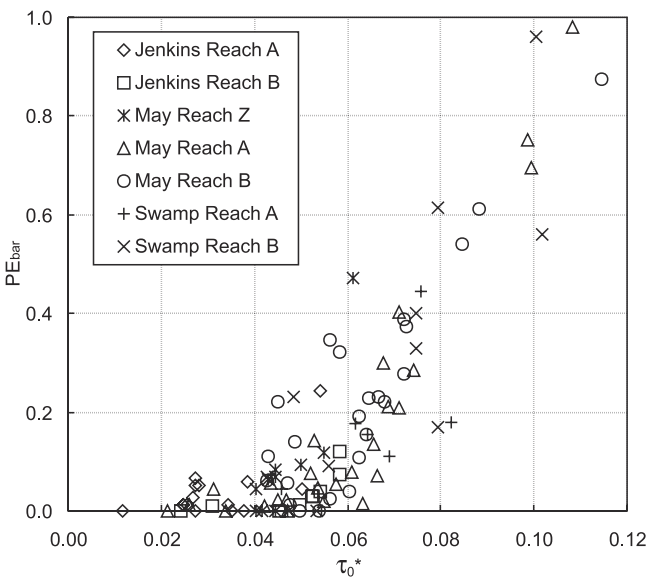

Figure 8. Fraction of bed tags missing (PE_{bar}) from seven gravel bars during floods as a function of peak dimensionless shear stress τ_0^*.

Table 2. Fraction of Bed Tags Missing (PE_{bar}) During Inventories[a]

	Jenkins Creek			May Creek		Swamp Creek	
Inventory Date	Bar A	Bar B	Bar Z	Bar A	Bar B	Bar A	Bar B
10 Nov. 1997	N	N	N	0.14	N	N	N
18 Nov. 1997	N	N	N	0.06	N	N	N
20 Nov. 1997	N	N	N	0.02	N	N	N
24 Nov. 1997	N	N	N	0.01	N	N	N
2 Dec. 1997	N	N	N	0.02	N	N	N
4 Dec. 1997	N	N	N	0.00	N	N	N
10 Dec. 1997	N	N	N	0.01	N	N	N
12 Dec. 1997	0.08	N	N		N	N	N
17 Dec. 1997	0.05	N	N		N	N	N
19 Dec. 1997		N	N	0.21	0.22	N	N
1 Jan. 1998	0.03	N	N	0.08	0.06	N	N
8 Jan. 1998		N	N	0.40	0.39	N	N
13 Jan. 1998	0.07	N	N			N	N
18 Jan. 1998		N	N	0.21	0.28	N	N
3 Feb. 1998	0.05	N	N	0.07	0.15	N	N
5 March 1998	0.01	N	N	0.05	0.22	N	N
25 March 1998	0.01	N	N	0.05	0.00	N	N
4 May 1998		N	N	0.00	0.11	N	N
16 Nov. 1998			N			0.04	0.07
17 Nov. 1998	0.00	0.00	N	0.00	0.00		
21 Nov. 1998	0.01	0.01	N	0.04	0.35		
28 Nov. 1998			N	0.98	0.87		
29 Nov. 1998	0.24	0.12	N				
3 Dec. 1998			N	0.08	0.32		
7 Dec. 1998	0.06	0.01	N				
11 Dec. 1998			N	0.02	0.01		
15 Dec. 1998			N			0.44	0.96
23 Dec. 1998			N	0.70	0.61		
31 Dec. 1998			0.47	0.75	0.54		
4 Jan. 1999	0.04	0.07				0.18	0.23
25 Jan. 1999	0.00	0.04	0.06	0.30	0.19		
27 Jan. 1999						0.16	0.40
11 Feb. 1999			0.04	0.14	0.11		
12 Feb. 1999	0.00	0.03				0.11	0.33
8 March 1999						0.18	0.61
9 March 1999	0.01	0.03	0.09	0.28	0.23		
31 March 1999	0.00	0.00	0.00	0.01	0.03	0.00	0.00
10 Nov. 1999	N	N	0.12	N	0.06	N	
12 Nov. 1999	N	N		N		N	0.00
16 Nov. 1999	N	N	0.08	N	0.37	N	0.56
29 Nov. 1999	N	N	0.07	N	0.14	N	0.09
13 Dec. 1999	N	N	0.00	N	0.04	N	0.17
17 Dec. 1999	N	N	0.00	N	0.33	N	0.00

[a] N indicates no bed tags were installed at the bar.

which all tags were observed to be stable was higher than the minimum value of τ_0^* at which some tags moved at that bar (Table 3). The minimum values of τ_0^* for which at least one tag moved ranged from 0.025 to 0.046 among the bars. The maximum values of τ_0^* at which all tags were stable ranged from 0.038 to 0.053 among the bars.

[44] The lack of a clear threshold of bed material entrainment at each of the gravel bars may be a result of sampling error, changes in the strength of the bed, or the stochastic interactions between streamflow and the streambed. As noted, there may have been bed material movement along a bar even if no bed tag was missing. In the case of type 1 error the maximum reported values of τ_0^* for a stable bed in Table 3 may be too high. The strength of the bed surface may have changed over time as a result of the transport and deposition of bed material. If the particle size distribution of the bed surface had changed, the apparent variation in τ_{cr}^* over time would be an artifact of failing to update the D_{50} from flood to flood. Moreover, structural changes in the bed surface, not accompanied by changes in its particle size distribution, may account for variation in τ_{cr}^* of the bed over time. Finally, there may have been differences in how the applied shear stress was distributed over the streambed due to velocity fluctuations in turbulent streamflow that produced bed material entrainment during one event but not another. In this case, bed material entrainment represents a stochastic process.

5.2. Variation in Partial Entrainment for a Given Shear Stress at a Bar

[45] The value of PE_{bar} at a specified value of τ_0^* varied between inventories at individual sites as shown by the vertical scatter within the data for Jenkins A, May A, May B, and Swamp B (Figure 8). As with the threshold of entrainment, the variation in partial entrainment at a given shear stress may be a result of sampling and measurement error, changes in the strength of the bed surface, or the stochastic distribution of the applied shear stress during floods. Sampling error due to the bed tags (i.e., the vertical

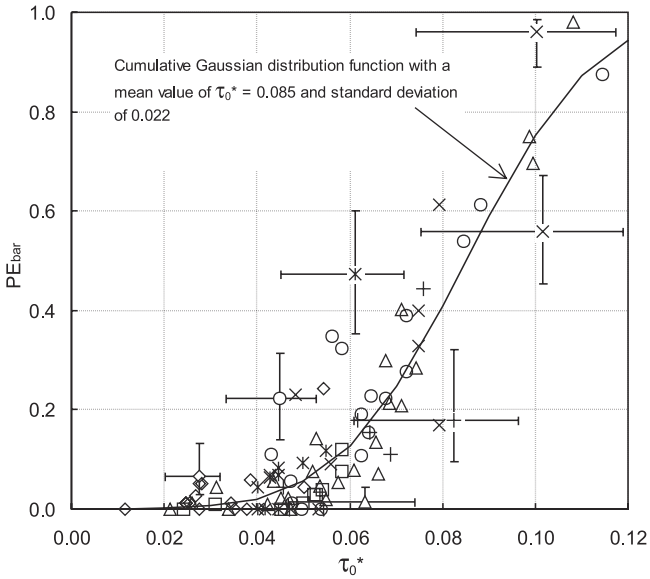

Figure 9. Cumulative Gaussian distribution function (solid line) with fraction of bed tags missing (PE_{bar}) from gravel bars as a function of peak dimensionless shear stress τ_0^* and examples of 95% confidence intervals for selected observations.

error bars in Figure 9) might account for some of the observed variation in PE_{bar} at a site for a given value of τ_0^*, but it is unlikely to account for all of the variation. Here τ_0^* has a margin of error related to the hydraulic calculations, the estimate of D_{50}, and the approximation of τ_g by τ_0. These errors are likely to introduce a uniform bias for floods of similar magnitudes at a site, so they are unlikely to account for variation over time in the relation between PE_{bar} and τ_0^* at a site.

[46] Variation in PE_{bar} for a given value of τ_0^* also may represent actual differences in the spatial extent of bed material entrainment that could arise because of variable flood durations or changes in bed surface strength during floods. First, partial entrainment may vary with the duration of a flood, which is not represented by τ_0^*. For example, inventories conducted after multiple flood peaks indicate higher values of PE_{bar} relative to τ_0^* than inventories conducted after a single flood peak. The hydrograph for Swamp Creek (Figure 7) shows three distinct peaks in discharge rate for the period prior to the 15 December 1998 inventory, whereas there was only one peak for the period prior to the 16 November 1999 inventory. As a result, the inventory on 15 December 1998 had a larger fraction of tags missing ($PE_{bar} = 0.96$) than the 16 November 1999 inventory ($PE_{bar} = 0.56$), even though τ_0^* was 0.10 for both inventories (Figure 7). The value of PE_{bar} for an inventory after F flood peaks can be calculated assuming independent entrainment of bed tags from flood to flood as

$$PE_{bar} = 1 - \prod_{f=1}^{F} \left(1 - PE_{barf}\right), \quad (7)$$

where $1 - PE_{barf}$ is the fraction of the bar that was stable in the fth flood. In the Swamp Creek example the expected value of PE_{bar} for the 15 December 1998 inventory was calculated using equation (7) by setting PE_{barj} equal to 0.75, the expected value of PE_{bar} for a single flood when $\tau_0^* = 0.10$ based on equation (3), for each of the three peaks ($F = 3$). The cumulative entrainment predicted from equation (6) is 0.98 compared to an observed value of 0.96.

[47] In contrast, PE_{bar} at the Jenkins Creek sites for two flood peaks between 7 December 1998 and 4 January 1999 is lower than PE_{bar} for a previous flood in November 1998 of similar magnitude (Figure 7). We suggest that the difference between the streams may be related to the magnitude of the floods. In Swamp Creek the floods were capable of entraining over half of the bed surface, whereas the floods in Jenkins Creek were capable of entraining a quarter of the bed surface at most. Large floods may rearrange particles on the bed surface, equivalent to reshuffling a deck of cards, and maintain the independent selection of grains from the surface. Small floods, however, remove small and unconstrained particles such that the probability of entrainment is not independent from event to event.

[48] The potential influence of flow duration on partial entrainment was examined for May B. As an alternative to shear stress, stream power has been used to analyze sediment transport rates [*Bagnold*, 1977] and can be integrated over time to assess the work done by a river moving sediment. An index of the work per unit of streambed area for each inventory was calculated in discrete form as product of excess unit stream power ($\omega - \omega_c$) and time (900 s) summed over the period (t) since the previous inventory:

$$\Phi = 900 \sum_{t} (\omega - \omega_c)^{3/2}, \quad (8)$$

where $\omega = \gamma_w QS/w$, w is channel width, $\omega_c = 9.8$ W m^{-2} (1 kg m^{-1} s^{-1}), and Q is the mean discharge rate for the 15-min period t. There was more variation in the relation between PE_{bar} and Φ than τ_0^* particularly at intermediate levels of partial entrainment (Figure 10). Thus flow duration may explain the variation in PE_{bar} for a given τ_0^* where multiple, large floods occurred (e.g., the inventory on 15 December 1998 for Swamp B), but it is unlikely to be a dominant source of the variation.

Table 3. Peak Reach Average Dimensionless Shear Stress τ_0^* Bracketing Initial Motion Conditions

Site	Maximum τ_0^* When No Tags Were Missing	Minimum τ_0^* When at Least One Tag Was Missing (Percent of Tags Missing)
	Jenkins Creek	
Bar A	0.038	0.026 (1%)
Bar B	0.052	0.039 (1%)
	May Creek	
Bar A	0.038	0.025 (1%)
Bar B	0.053	0.042 (1%)
Bar Z	0.045	0.040 (4%)
	Swamp Creek	
Bar A	0.047	0.046 (4%)
Bar B	0.048	0.038 (7%)

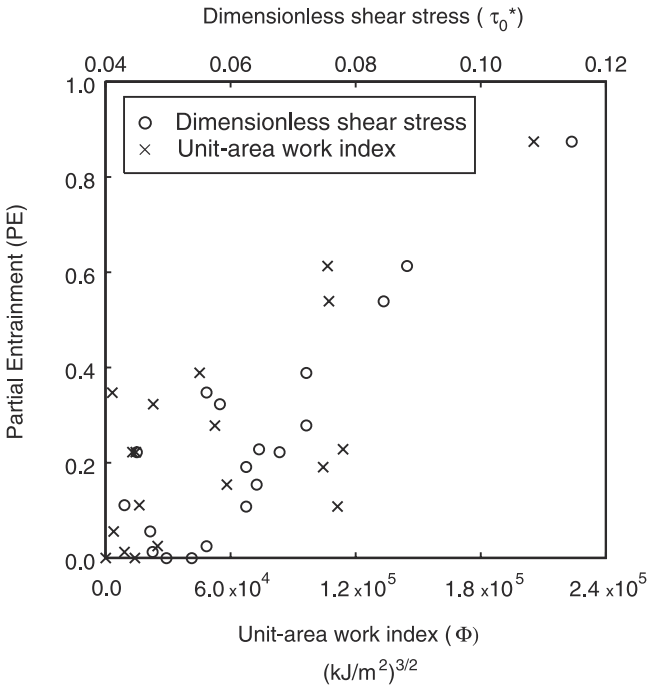

Figure 10. Relations of partial entrainment (PE) to unit area work index and dimensionless shear stress at May B. Unit area work index is $\Sigma(\omega - \omega_{cr})^{3/2}$, where ω is unit area stream power and $\omega_{cr} = 9.8$ W m^{-2}.

[49] Instead, streamflow is likely to modify the structure of the bed surface or its particle size distribution between inventories, resulting in variation in PE_{bar} for a given value of τ_0^* over time. Flow-mediated changes in the strength of the bed surface were analyzed for pairs of inventories at a site when τ_0^* differed by no more than 0.005. Values of PE_{bar} for the pairs were tested to determine if they were likely to represent two outcomes of floods with the same probability of entrainment. For each pair the cumulative binomial distribution function equation (5) was applied iteratively to find the entrainment probability p at which the likelihood, $B(N)$, of the two observed values of PE_{bar} were equal. (Here p is approximately equal to the mean of the observed values of PE_{bar} for the pair of inventories.) When the likelihood of observing the two values of PE_{bar} was <5%, given p, the two inventories were considered to be significantly different.

[50] There were six pairs of inventories where τ_0^* was equal for the two inventories in the pair but the values of PE were significantly different. These inventories occurred at four gravel bars (Jenkins A, May A, May B, and Swamp B) (Table 4). In five of the pairs, PE_{bar} for the first inventory was greater than PE_{bar} for the second inventory, which represents an increase in bar strength over time. The greatest increase in bar strength occurred at Swamp B where PE_{bar} decreased from 0.61 to 0.17 for two floods when τ_0^* was 0.082. Other inventories show a pattern of increasing bed stability over time, though the differences in PE_{bar} were not statistically significant.

[51] Only one pair of inventories showed a significant increase in the extent of bed material entrainment over a pair of floods with similar magnitudes. At May B, PE_{bar} was 0.06 when τ_0^* was 0.046 for a flood on 1 January 1998; PE_{bar} was 0.22 when τ_0^* was 0.044 for a flood on 5 March 1998. Between January and March 1998, there were three intervening floods, with values of PE_{bar} ranging from 0.15 to 0.39, that may have modified the structure or texture of the bed surface at May B.

6. Influence of Past Floods on Partial Entrainment During Intermediate Magnitude Floods

[52] Flow-mediated changes in the strength of bar surfaces were further analyzed in terms of the influence of past floods on partial entrainment for all floods when τ_0^* was 0.055 to 0.070 (Table 5). We hypothesized that after large floods, the bed surface would be relatively weaker (e.g., because an armored surface was breached but not reestablished) than after an intermediate flood. Under this hypothesis we posit that recessional flows from a single, large flood would not be sufficient to reestablish an armor layer. As a result, partial entrainment for a flood when $0.055 < \tau_0^* < 0.070$ would be higher when the previous flood was large than partial entrainment for other floods when $0.055 < \tau_0^* < 0.070$. Furthermore, intermediate-magnitude floods would strengthen the bed surface, so that partial entrainment for a flood when $0.055 < \tau_0^* < 0.070$ would be lower than expected when the previous flood was of intermediate magnitude.

[53] The analysis compared values of PE for intermediate magnitude floods to the strength of the previous flood within that season. We selected only inventories when τ_0^* ranged from 0.055 to 0.070 because the variation of PE_{bar} was large (from 0 to 0.48) among these inventories but not strongly related to the variation in τ_0^* (Figure 8). The inventories were

Table 4. Significantly Different Values of Partial Entrainment (PE_{bar}) at a Site for Floods of Similar Magnitude

Site	First Inventory			Second Inventory			Probability of Entrainment for Equal Likelihood of Observed Values of PE_{bars}
	Date	τ_0^*	PE_{bar}	Date	τ_0^*	PE_{bar}	
Jenkins A[a]	29 Nov. 1998	0.056	0.24	4 Jan. 1999	0.052	0.04	0.13
May A[a]	8 Jan. 1998	0.073	0.4	18 Jan. 1998	0.073	0.21	0.30
Swamp B[a]	4 Jan. 1999	0.045	0.23	12 Nov. 1999	0.047	0.00	0.10
Swamp B[a]	8 March 1999	0.082	0.61	13 Dec. 1999	0.082	0.17	0.38
May A[a]	25 Jan. 1999	0.070	0.30	11 Feb. 1999	0.068	0.14	0.22
May B[b]	1 Jan. 1998	0.046	0.06	5 March 1998	0.044	0.22	0.14

[a] Increase in bed stability over time.
[b] Decrease in bed stability over time.

Table 5. Partial Entrainment for Inventories When $0.055 < \tau_0^* < 0.070$ Illustrating the Influence of Previous Floods on Bed Stability

	Group A	Group B	Group C	Group D
Dimensionless shear stress of previous flood τ_p^*				
Mean of group	0.043	0.062	0.07	0.10
Range of group	0.026–0.054	0.060–0.064	0.065–0.074	0.084–0.115
Number of inventories	8	6	5	5
Mean dimensionless shear stress for inventories in group τ_0^*	0.060	0.064	0.063	0.061
Partial entrainment, PE_{bar}	0.143	0.142	0.080	0.196

divided into four groups on the basis of the value of the peak dimensionless shear stress for the previous inventory (τ_p^*). Inventories when $0.026 < \tau_p^* < 0.054$ were in group A. Inventories when $0.060 < \tau_p^* < 0.064$ were in group B. Inventories when $0.065 < \tau_p^* < 0.074$ were in group C. Inventories when $0.084 < \tau_p^* < 0.115$ were in group D.

[54] The mean value of PE_{bar} for all inventories when $0.055 < \tau_0^* < 0.070$ was 0.15. The mean value of PE_{bar} for groups A and B was 0.14, for group C was 0.08, and for group D was 0.20. Only groups C (previous flood had an intermediate magnitude) and D (previous flood with a high magnitude) were significantly different ($p < 0.05$ based on a one-tailed Student's t distribution). The results demonstrate higher bed strength (lower PE_{bar}) after intermediate-magnitude flows ($0.065 < \tau_0^* < 0.074$) and lower bed strength (higher PE_{bar}) after high flows ($\tau_0^* > 0.84$).

[55] Changes in the strength of the streambed at the sites were not associated with any significant changes (<5 mm) in the median diameter of bed material from summer to summer. There may have been transient changes in bed material texture between storms [e.g., *Gomez*, 1983a] that were not evident from the results of pebble counts conducted during periods of lower flow. Bed strength also may have increased as particles were moved into more stable positions without detectable changes in the particle size distributions over time.

7. Spatial Uniformity of Bed Material Entrainment

[56] The hypothesis that the probability of entrainment is uniform over a gravel bar during a flood was tested by comparing the fraction of bed tags missing for a bar (PE_{bar}) to the fraction of tags missing from each row in the bar (PE_{row}). There were 372 PE_{bar}, PE_{row} pairs for which at least one tag was missing from the gravel bar. The pairs are plotted in Figure 11. For each pair the probability of observing PE_{row} given PE_{bar} was determined using the cumulative binomial distribution equation (5), where p is equal to PE_{bar}, n is the number of tags in the row, and N is the number of tags missing from that row (i.e., $N/n = PE_{row}$).

[57] Most observations of PE_{row} (341 or 92%) were within the 95% confidence interval around PE_{bar} (circles in Figure 11). However, PE_{row} differed significantly from PE_{bar} for 31 instances (crosses in Figure 11). There were 10 instances when the fraction of tags entrained at a row was significantly less than fraction entrained at the bar (PE_{row} was below the confidence intervals for PE_{bar}) and 21 instances when the fraction of tags entrained at a row was significantly greater than the fraction entrained at the bar. The anomalously low and high values of PE_{row} were distributed among 16 rows at all of the sites, except Swamp A, and occurred during periods with both high and low levels of partial entrainment.

[58] At six rows, PE_{row} was significantly different than PE_{bar} for more than one inventory. Values of PE_{row} were less than PE_{bar} at two of the rows (May A.5 and Swamp B.1). These relatively stable rows were located in regions of divergent flow where the channel widened slightly downstream. Values of PE_{row} were greater than PE_{bar} at four of the rows (May A.7, A.10, and B.3 and Swamp B.3). These less stable rows were in regions of converging flow (May A.7 and B.3) and along the foreset slope of a bar (May A.10 and Swamp B.3).

[59] The uniform probability hypothesis was also tested for a reach spanning the bar at May A and including portions of a downstream pool (Figure 3). As with the analysis of the bars, preferential entrainment and stability of rows in May Reach A was evaluated using the cumulative binomial distribution function equation (5) to calculate the probabil-

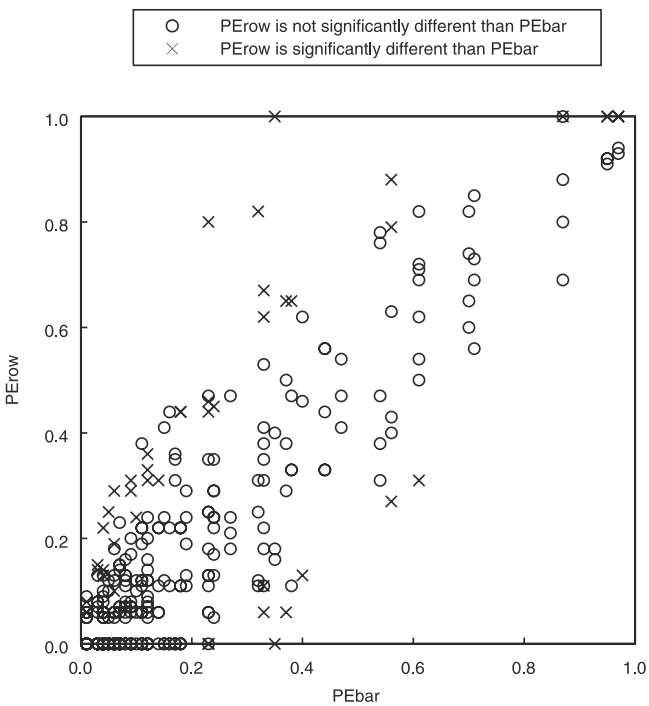

Figure 11. Comparison of partial entrainment at rows (PE_{row}) and bars (PE_{bar}), where crosses indicate that the probability of entrainment at a row was unlikely ($p < 0.05$) to be equal to the probability of entrainment for the surrounding bar.

ities of the observed numbers of tags missing from or present in individual rows given the reach average probability of tags missing during WY 1998. In this application, n is the number of tags in a row, N is the number of tags stable throughout the winter in that row, and p is the fraction of tags that were stable throughout the winter in the reach.

[60] In May Reach A, preferential instability at rows 9 and 12 and stability at row 5 are evident from the fraction of tags stable throughout the period from December 1997 to March 1998. Thirty-five percent of all tags in the May Reach A were stable throughout this period, but only 12% of tags were stable in row 7 and 6% were stable in row 10 ($p < 0.05$ that the stable fraction of the bed at the rows was equal to 35%). In contrast, 72% of the tags in rows 5 and 56% of the tags in row 6 were stable throughout WY 1998 ($p < 0.05$ that the stable fraction of the bed at these rows was equal to 35%).

[61] The least stable rows in May Reach A are located upstream of hydraulic controls during low flow (Figure 3). The crest of a transverse bar forms the low-flow hydraulic control downstream of row 9, while the tail end of a pool forms the low-flow hydraulic control downstream of row 12. As a result of the backwater formed upstream of the controls, the current velocity is slightly less and the bed material is finer grained at these sections than for most of the reach (D_{50} = 30 and 27 mm for pebble counts along rows 9 and 12, respectively). As stage increases in this reach, the downstream sections no longer act as a hydraulic control, and the water surface slope and current velocities increase at rows 9 and 12 to levels representative of the reach as a whole. As a result, bed material entrainment is more extensive during higher flows at these sections than for the bed as a whole.

[62] In contrast, the most stable rows (5 and 6) in the reach are located on a shallow foreset slope of a bar. The bed material is relatively coarse in these sections (D_{50} = 42 mm for pebble count between rows 5 and 6), reflecting relatively high shear stress values at low and intermediate stages. The patterns of stability at these rows indicate that the local particle size distribution of the bed surface may be set by size-selective deposition and transport during intermediate and lower flows.

8. Spatial Independence of Bed Material Entrainment

[63] The independence of the location of bed material entrainment at the scale of a gravel bar is analyzed for the series of inventories at all sites, except May Z. For a series of I inventories the number of times that a bed tag was missing from a location on a bar can range from 0 to I. We calculated the number of times tags were missing from each location for the inventories conducted during WY 1999. The results are aggregated as a histogram for each bar of the number of locations $L(j)$ where bed tags were missing j times. The sum of $L(j)$ for $j = 0$ to I is the total number of tag locations on the bar. We tested the hypothesis of the spatial independence of bed material entrainment by comparing these observed distributions to the expected distributions if the location of missing bed tags was independent from flood to flood.

[64] The probability distribution for the frequency that bed tags were missing from a location on a bar was calculated assuming that the entrainment probability is uniform over the bar and equal to the observed value of PE_{bar} for each inventory. We begin by considering the sequence of observations that a tag was present or missing for a series of I inventories at a single tag location on a gravel bar: $\{OB_1, OB_2, \ldots, OB_I\}$. If a tag was missing for the ith inventory then $OB_i = 0$; if the tag was present then $OB_i = 1$. There are 2^I possible sequences of observations for i inventories at a given tag location on a bar. For an example, there are four possible sequences of observations for two inventories at any location: {0,0}, {0,1}, {1,0}, or {1,1}.

[65] The probability that tags were missing j times from a location is equal to the sum of the probabilities of all possible sequences when a tag was missing j times. The probability of a particular sequence of observations is the product of the individual probabilities p_i of each observation in the sequence. For spatially independent bed material entrainment we assumed the probability that a tag was missing from a location on a gravel bar was equal to the observed partial entrainment and the probability a tag was present was equal to the complement of partial entrainment: $p_i = PE_{bar}$ for $OB_i = 0$ and $p_i = 1 - PE_{bar}$ for $OB_i = 1$.

[66] We calculate the probability $P(j)$ that a tag was missing for j out of I inventories using

$$P(j) = \sum_{S} \left[\prod_{i=1}^{I} p_i \right], \tag{9}$$

where S is the set of sequences when a tag was missing j times. The result is the probability distribution for the frequency j that tags were missing from a location (i.e., the histogram of $P(j)$ for $j = 0$ to I). The product $nP(j)$ gives the expected number of locations that bed tags were missing j times for a bar with n tags if the location of bed material entrainment is independent from flood to flood.

[67] We assessed the likelihood of the observed distribution of the number of locations where tags were missing j times, $L(j)$, to the distribution, $P(j)$, predicted from equation (9) for each bar using a χ^2 test [*Helsel and Hirsch*, 1993]. To satisfy conditions for using the test [*Hoel*, 1971], the frequency classes j of the distributions were aggregated into larger classes (e.g., j = 0 − 2 inventories for the first class, 3–4 inventories for the second class, . . .) so that there were at least five observed or predicted locations in each frequency class.

[68] The application of equation (9) to May B is used as an example. May B had 11 bed tag inventories during WY 1999. At any location on the bar a bed tag may have been present during all 11 inventories or missing for as many as 10 of the inventories (no tags were missing for one inventory). The mode of both the observed and predicted distributions, $L(j)$ and $nP(j)$, was $j = 3$ inventories when tags were missing (Figure 12). Tags were missing for three inventories at 22 of the 85 tag locations on May B ($L(j) = 22$ for $j = 3$). We calculated that there was a 32% probability that tags were missing from a location for three inventories if bed material entrainment was spatially independent from flood to flood ($P(j) = 0.32$ for $j = 3$). Thus we expected that 27 of the 85 tag locations would have had tags missing for three inventories during WY 1999 at May B.

[69] The observed distribution at May B has more "stable" locations (i.e., those where tags were missing for 0 or 1

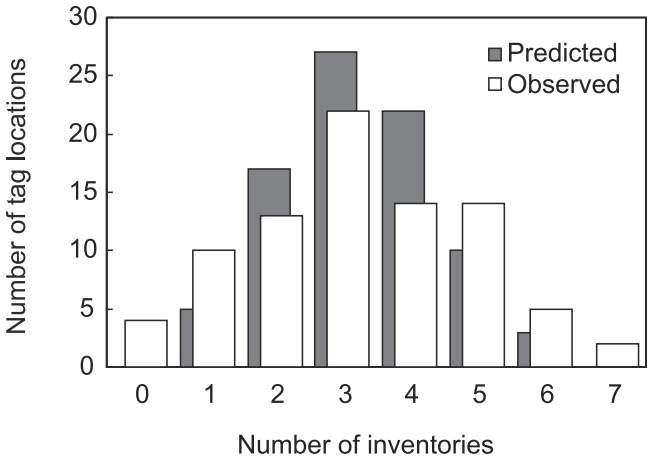

Figure 12. Predicted and observed distributions of the number of inventories that bed tags were for the 85 tag locations at May B.

inventories) and more ''unstable'' locations (i.e., those where tags were missing for 5, 6, or 7 inventories) than would be expected if the probability of bed material entrainment were uniform along the bar for each flood. Likewise, there were fewer locations with intermediate stability (i.e., those where tags were missing for 2, 3, or 4 inventories).

[70] The most stable bed tag locations in May B were near the banks and sections of diverging flow (Figure 13). The unstable locations were near the center of the channel and in sections of converging flow. These patterns do not correspond to the textural variation along the bar: May B.1 (farthest upstream section) had the finest-grained material (D_{50} = 27 mm) of any section of the bar; regions of the bed along the stream banks generally had finer material than the bar as a whole, and May B.3 (immediately downstream of the log) had the coarsest material on the bar (D_{50} = 38 mm).

[71] The observed distributions at May A, May B, and Swamp B were significantly different than the predicted distributions ($p < 0.001$) and, as described for May B, were more variable. The differences between the observed and predicted distributions indicate that the location of bed material entrainment was not independent from flood to flood at these bars. Instead, regions of higher and lower probabilities of entrainment emerge over a series of floods.

[72] The independence of the location of bed material entrainment cannot be rejected for Jenkins A, Jenkins B, May Z, or Swamp A. At these sites, however, bed tags were missing from any location at most for three inventories. The independence of the location of bed material entrainment is apparently a reasonable approximation for three or fewer floods, particularly when the flood are large as demonstrated by cumulative extent of bed material entrainment at Swamp B between 16 November and 15 December 1998.

9. Application of Bed Tags

[73] A variety of techniques have been used to document spatial patterns in the entrainment of streambed material including tracer particles, distributed bed load traps, and videography. Bed tags provide an alternative method for documenting the entrainment of material deposited by a stream and analyzing bed material entrainment from a Eulerian reference frame. The results of the bed tag inventories are influenced by the size of tag relative to the feature of interest. In this investigation the diameter of the bed tags represents the approximate vertical length scale of the contacts between particles forming the surface of the streambed. A bed tag appreciably larger than this length would be supported by the contacts between subsurface particles and thus would be less sensitive to movement of surface particles. Smaller tags, however, are likely to produce similar results as long as the tag is supported by the contact between surface particles, as was demonstrated by the wire-tag design.

[74] Bed tags would not be an appropriate method for some questions and situations. They do not indicate low levels of bed material entrainment as would be expected for a widely graded, poorly sorted sediment regardless of whether the particles were segregated into different textural patches or well mixed. Likewise, bed tags are inappropriate for documenting a bed covered by many unconstrained particles, where the center of mass of each particle is well above their contact points with other particles. Although deposition without entrainment was documented infrequently at these sites, it may be a dominant indicator of sediment transport and bed disturbance at other sites. In this case, burial of bed tags could be recorded and analyzed.

10. Bed Material Entrainment in Gravel Bed Streams

[75] At the scale of a gravel bar, spatially distributed values of τ and τ_{cr} produce approximately random entrainment where the partial entrainment of the bed is normally distributed with respect to the τ_0^*. The zone of active bed load transport is not a contiguous region at the center of the channel that expands with flood magnitude. Instead, floods entrain bed material stochastically from widely distributed locations over a gravel bar's surface. Over a longer series of floods, however, regions of preferential stability and instability emerge: there is a higher probability of bed material entrainment in the center of the channels and at sections with convergent flow than near the channel banks. Because of these patterns, scaling of event probabilities by assuming independence over time will produce erroneous estimates of the cumulative entrainment of a streambed or the frequency

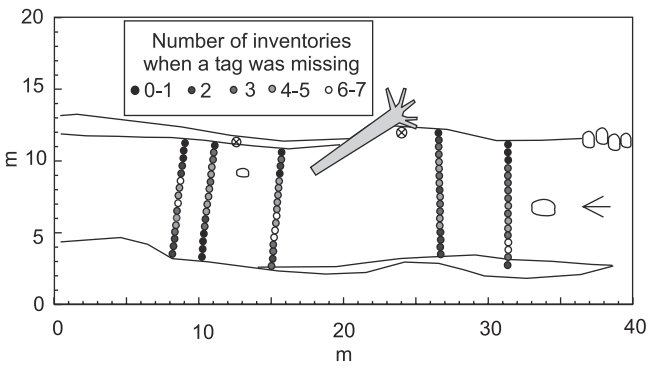

Figure 13. Frequency that tags were missing from locations in May B during WY 1998.

of entrainment at a location over multiple flood events. In these cases, additional information about flow-mediated changes in the strength of the bed and the spatial distributions of τ and τ_{cr} are needed to assess sediment supply for bed load transport and streambed disturbance over periods greater than individual floods.

[76] Intermediate-magnitude floods appear to strengthen bar surfaces, perhaps by removing small and unconstrained particles from the streambed, rearranging particles into more stable structures, and depositing large particles. As a consequence, the probability of bed material entrainment is not independent from event to event but, instead, declines over a series of small to intermediate events. Streamflow is likely to produce this effect only in gravel bed streams where the sediment supply is limited.

[77] Floods begin to weaken the bed surface when they entrain ~50% of a bar's surface. Under such a condition, bed material is transported indiscriminately with respect to particle size such that the bed surface is unlikely to armor or otherwise form stable structures [*Little and Mayer*, 1976; *Garde et al.*, 1977; *Gomez*, 1983a, 1983b; *Shen and Lu*, 1983; *Kuhnle and Southard*, 1988; *Hassan and Reid*, 1990; *Chin et al.*, 1992]. In contrast to small and intermediate floods, large floods maintain the spatial independence of bed material entrainment by transporting particles without regard to their size and rearranging much of the bed surface.

[78] The influence of flow duration on partial entrainment remains to be tested thoroughly as the duration of floods could not be controlled in these unregulated streams. *Wilcock and McArdell* [1997] observed that the active portion of a bed increases over time reach a constant at a timescale dependent on the transport rate and bed length. They suggested that the timescale may be longer than the duration of high flows in many streams. In this case, PE_{bar} would be influenced by flow duration. Indeed, cumulative values of PE_{bar} increased over multiple flood events in some cases. However, the decline in PE_{bar} over time and the spatial dependence of bed material entrainment indicates that the active portion of the bed may attain an equilibrium value over a period of multiple floods in streams until a large event reorders particles. Partial entrainment does not vary strongly with stream power integrated over time. In this way, patterns of bed material entrainment are unlike sediment transport rates, which can be maintained by a small population of active particles and thus are likely to related to stream power.

11. Conclusions

[79] Most floods in gravel bed streams entrain only a portion of the material forming the streambed surface. The partial entrainment of streambed provides an estimate of the probability of entrainment. In this investigation of seven gravel bars in three streams the partial entrainment of gravel bars had a Gaussian distribution with respect to the peak τ_0^* of a flood. The distribution had a mean value of $\tau_0^* = 0.085$ (at which 50% of a bar's surface is expected to be entrained), a standard deviation of 0.022, and a root-mean-square error of 9% of a bar's surface compared to observed partial entrainment. Partial entrainment was not consistently related to the return period of a flood among the streams: PE_{bar} for a 2.5-year event varied from <10% in Jenkins Creek to >90% in May Creek.

[80] The simple stochastic relation between τ_0^* and partial entrainment provides a means for calculating the extent of disturbance during a flood of a gravel streambed comprising a single particle size distribution (either unimodal or bimodal) and uniform flow conditions. The relation can also serve as an event-scale probability of entrainment for estimating the sediment supplied from a streambed to bed load transport.

[81] The variation in partial entrainment of a gravel bar at a given value of τ_0^* may result from the low precision of PE_{bar} estimates, the failure of τ_0^* to account for the cumulative entrainment of the streambed over a period of time (particularly for multiple floods), or flow-mediated changes in the strength of the bed surface. The transition between floods that strengthened the bed surface from the larger floods that weakened the bed occurred at a value of τ_0^* of ~0.08, when ~50% of a bar's surface would be entrained.

[82] The probability of bed material was approximately uniform over a gravel bar during a flood, provided the bar had uniform sedimentologic and hydraulic conditions. Bed material entrainment is only approximately independent from flood to flood, particularly during and after large floods that entrain 50% or more of a bar. In contrast, the probability of entrainment declined for a series of consecutive small and intermediate magnitude floods. Bed material near the center of a channel and in laterally or vertically convergent sections was likely to be entrained more frequently than the material near the channel banks and in sections of divergent streamflow over the course of a wet season. The deviations from uniform and independent bed material entrainment prevent simple scaling of event probabilities over periods spanning multiple floods to estimate the supply of material for bed load transport or the cumulative extent of streambed disturbance.

[83] **Acknowledgments.** This work was supported in part by the U.S. Environmental Protection Agency, Water and Watersheds Program under agreement R82-5484-010. Suggestions by Ned Andrews, John Pitlick, and two anonymous reviewers were greatly appreciated.

References

Andrews, E. D., Entrainment of gravel from naturally sorted riverbed material, *Geol. Soc. Am. Bull.*, *94*, 1225–1231, 1983.

Andrews, E. D., Marginal bed load transport in a gravel bed stream, Sagehen Creek, California, *Water Resour. Res.*, *30*, 2241–2250, 1994.

Andrews, E. D., and D. C. Erman, Persistence in the size distribution of surficial bed material during an extreme snowmelt flood, *Water Resour. Res.*, *22*, 191–197, 1986.

ASCE Task Committee on the Sedimentation Manual, Sediment transportation mechanics: initiation of motion, *J. Hydraul. Div. Proc. Am. Soc. Civ. Eng.*, *92*, 291–314, 1996.

Ashworth, P. J., and R. I. Ferguson, Size-selective entrainment of bed load in gravel bed streams, *Water Resour. Res.*, *25*, 627–634, 1989.

Bagnold, R. A., Bed load transport by natural rivers, *Water Resour. Res.*, *13*, 303–312, 1977.

Brayshaw, A. C., L. E. Frostick, and I. Reid, The hydrodynamics of particle clusters and sediment entrainment in coarse alluvial channels, *Sedimentology*, *30*, 137–143, 1983.

Buffington, J. M., and D. R. Montgomery, A systematic analysis of eight decades of incipient motion studies, with special reference to gravel-bedded rivers, *Water Resour. Res.*, *33*, 1993–2030, 1997.

Carling, P. A., Threshold of coarse sediment transport in broad and narrow natural streams, *Earth Surf. Processes Landforms*, *8*, 1–18, 1983.

Chin, C. O., B. W. Melville, and A. J. Raudkivi, Streambed armoring, *J. Hydraul. Eng.*, *120*, 899–917, 1992.

Chow, V. T., *Open Channel Hydraulics*, McGraw-Hill, New York, 1959.

Church, M., D. Jones, Channel bars in gravel-bed rivers, in *Gravel-Bed Rivers*, edited by R. D Hey, J. C. Bathurst, and C. R. Thorne, pp. 291–338, John Wiley, New York, 1982.

Diplas, P., and A. J. Sutherland, Sampling techniques for gravel sized sediments, *J. Hydraul. Eng.*, *114*, 484–501, 1988.

Einstein, H. A., Formulas for the transportation of bed load, *Trans. Am. Soc. Civ. Eng.*, *107*, 133–149, 1942.

Einstein, H. A., The bed-load function for sediment transportation in open channel flows, *Soil Conserv. Serv. Tech.*, *1026*, 1950.

Einstein, H. A., and N. L. Barbarossa, River channel roughness, *Trans. Am. Soc. Civ. Eng.*, *117*, 1121–1146, 1952.

Fahnstock, R. K., Morphology and hydrology of a glacial stream—White River, Mount Rainer Washington, *U.S. Geol. Surv. Prof. Pap.422A*, 70 pp., 1963.

Fenton, J. D., and J. E. Abbot, Initial movement of grains on a stream bed: The effect of relative protrusion, *Proc. R. Soc. London, Ser. A*, *352*, 523–537, 1977.

Garde, R. J., K. A. Ali, and S. Diette, Armoring processes in degrading streams, *J. Hydraul. Div. Proc. Am. Soc. Civ. Eng.*, *103*, 1091–1095, 1977.

Gessler, J., Self-stabilizing tendencies of alluvial channels, *J. Waterw. Harbor Div. Am. Soc. Civ. Eng.*, *96*, 235–249, 1970.

Gilbert, G. K., The transportation of debris by running water, *U.S. Geol. Surv. Prof.*, *86*, 1914.

Gomez, B., Temporal variations in the particle-size distribution of surficial bed material: The effect of progressive bed armoring, *Geogr. Ann.*, *65A*, 183–191, 1983a.

Gomez, B., Temporal variation in bedload transport rates: The effects of progressive bed armouring, *Earth Surf. Processes Landforms*, *8*, 41–54, 1983b.

Grass, A. J., Initial instability of fine bed sand, *J. Hydraul. Div. Proc. Am. Soc. Civ. Eng.*, *96*, 619–631, 1970.

Grass, A. J., Structural features of turbulent flow over smooth and rough boundaries, *J. Fluid Mech.*, *50*, 233–255, 1971.

Hassan, M. A., and I. Reid, The influence of microform bed roughness elements on flow and sediment transport in gravel bed rivers, *Earth Surf. Processes Landforms*, *15*, 739–750, 1990.

Helsel, D. R., R. M. Hirsch, *Statistical Methods in Water Resources*, Elsevier Sci., New York, 1993.

Hey, R. D., and C. R. Thorne, Accuracy of surface samples from gravel bed material, *J. Hydraul. Eng.*, *109*, 842–851, 1983.

Hoel, P. G., *Introduction to Mathematical Statistics*, John Wiley, New York, 1971.

Ikeda, H., F. Iseya, Experimental study of heterogeneous sediment transport, *Environ. Res. Cent. Pap. 12*, 50 pp., Univ. of Tsukuba, Tskuba, Japan, 1988.

Kellerhals, R., and D. I. Bray, Sampling procedures for a coarse fluvial sediments, *J. Hydraulics Division, Proceedings of the American Society of Civil Engineers*, *97*, 1165–1180, 1971.

Kirchner, J. W., W. E. Dietrich, F. Iseya, and H. Ikeda, The variability of critical shear stress, friction angle, and grain protrusion in water-worked sediments, *Sedimentology*, *37*, 647–672, 1990.

Komar, P. D., and Z. Li, Pivoting analyses of selective entrainment of sediments by shape and size with application to gravel threshold, *Sedimentology*, *33*, 425–436, 1986.

Kuhnle, R. A., and J. B. Southard, Bed load transport fluctuations in a gravel bed laboratory channel, *Water Resour. Res.*, *24*, 247–260, 1988.

Lane, E. W., and A. A. Kalinske, The relation of suspended to bed material in rivers, *Eos Trans. AGU*, *21*, 637–641, 1940.

Laronne, J. B., and M. A. Carson, Interrelationships between bed morphology and bed-material transport for a small, gravel-bed channel, *Sedimentology*, *23*, 67–85, 1976.

Lisle, T. E., J. M. Nelson, J. Pitlick, M. A. Madej, and B. L. Barkett, Variability in bed mobility in natural gravel-bed channels and adjustments to sediment load at local and reach scales, *Water Resour. Res.*, *36*, 3743–3755, 2000.

Little, W. C., and P. G. Mayer, Stability of channel beds by armoring, *J. Hydraul. Div. Proc. Am. Soc. Civ. Eng.*, *102*, 1647–1661, 1976.

McLean, S. R., S. R. Wolfe, and J. M. Nelson, Predicting boundary shear stress and sediment transport over bed forms, *J. Hydraul. Eng.*, *125*, 725–736, 1999.

Montgomery, D. R., and J. M. Buffington, Channel-reach morphology in mountain drainage basins, *Geol. Soc. Am. Bull.*, *109*, 596–611, 1997.

Nece, R. E., and J. D. Smith, Boundary shear stress in rivers and estuaries, *J. Waterw. Harbors Div. Am. Soc. Civ. Eng.*, *96*, 335–358, 1970.

Neill, C. R., and M. S. Yalin, Quantitative definition of beginning of bed movement, *J. Hydraul. Div. Proc. Am. Soc. Civ. Eng.*, *95*, 585–588, 1969.

Parker, G., and P. C. Klingeman, On why gravel bed streams are paved, *Water Resour. Res.*, *18*, 1409 –1423, 1982.

Pitlick, J., Flow resistance under conditions of intense gravel transport, *Water Resour. Res.*, *28*, 891–903, 1992.

Rouse, H., Critical analysis of open-channel resistance, *J. Hydraul. Div. Proc. Am. Soc. Civ. Eng.*, *91*, 1–25, 1965.

Schlichting, H., *Boundary-Layer Theory*, McGraw-Hill, New York, 1979.

Shen, H. W., and J. Lu, Development and prediction of bed armoring, *J. Hydraul. Eng.*, *109*, 611–629, 1983.

Smith, J. D., and S. R. McLean, Spatially averaged flow over a wavy surface, *J. Geophys. Res.*, *82*, 1735–1746, 1977.

Taylor, G. I., Statistical theory of turbulence parts I and II, *Proc. R. Soc. London, Ser. A*, *151*, 421–454, 1935.

White, C. M., The equilibrium of grains on the bed of a stream, *Proc. R. Soc. London, Ser. A*, *174*, 322–338, 1940.

Whiting, P. J., and W. E. Dietrich, Boundary shear stress and roughness over mobile alluvial beds, *J. Hydraul. Eng.*, *116*, 1495–1511, 1990.

Wiberg, P. L., and J. D. Smith, Velocity distribution and bed roughness in high-gradient streams, *Water Resour. Res.*, *27*, 825–838, 1991.

Wilcock, P. R., Estimating local bed shear stress from velocity observations, *Water Resour. Res.*, *32*, 3361–3366, 1996.

Wilcock, P. R., The components of fractional transport rate, *Water Resour. Res.*, *33*, 247–258, 1997.

Wilcock, P. R., and B. W. McArdell, Partial transport of a sand/gravel sediment, *Water Resour. Res.*, *33*, 235–245, 1997.

Wolcott, J. F., and M. Church, Strategies for sampling spatially heterogeneous phenomena: The example of river gravels, *J. Sediment. Petrol.*, *61*, 534–543, 1991.

Wolman, M. G., A method of sampling coarse river bed material, *Eos Trans. AGU*, *35*, 951–956, 1954.

D. B. Booth and S. J. Burges, Department of Civil and Environmental Engineering, University of Washington, Seattle, WA 98105, USA.

C. P. Konrad, U.S. Geological Survey, Tacoma, WA 98402, USA. (cpkonrad@usgs.gov)

D. R. Montgomery, Department of Earth and Space Sciences, University of Washington, Seattle, WA 98105, USA.